Ion Pairs of Crystal Violet in Sodium Bis(2-ethylhexyl)sulfosuccinate Reverse Micelles

Carla S. Oliveira,[†] Erick L. Bastos,[†] Evandro L. Duarte,[‡] Rosangela Itri,[‡] and Mauricio S. Baptista*,[†]

Departamento de Bioquímica, IQ-USP, São Paulo−SP, C.P. 26077, 05599-970, and Departamento de Física Aplicada, IF-USP, São Paulo−SP, C.P. 66318, 05315-970, Brazil

Received April 25, 2006. In Final Form: July 20, 2006

The interfacial localization and the ion pair formation of the positively charged dye crystal violet (CV) in sodium bis(2-ethylhexyl)sulfosuccinate reverse micelles (AOT RMs) were studied by several structural and spectroscopic techniques and by quantum chemical calculations. The size and shape of the AOT RMs in the presence of CV were investigated by small-angle X-ray scattering, showing that CV does not significantly change the RM structure. CV localization as a function of the water to surfactant molar ratio (w_0) was characterized by H^1 and ^{13}C NMR, indicating the close proximity of CV to the sulfosuccinate group of AOT at small and large w_0 values. These results were confirmed by calculation of magnetic shielding constants using the gauge-independent atomic orbital method with the HF/6-31G(d) basis set. Two different types of ion pairs between AOT and CV, i.e., contact ion pair (CIPs) and solvent-separated ion pair (SSIPs), were characterized by UV−vis spectroscopy and quantum chemical calculations using the semiempirical ZINDO-CI method. In nonpolar isotropic solvents CIPs are formed with an association constant (K_{ASSOC}) of 2×10^4 mol^{-1} L in isooctane and 750 mol^{-1} L in chloroform. In AOT RMs at low w_0, CV−AOT CIPs are also formed. By increasing w_0, there is a sharp decrease in the CIP association free energy, and SSIPs are formed. (CV^+)(H_2O)(AOT^-) SSIPs are stable in the AOT RM up to the largest w_0 tested ($w_0 = 33$).

Introduction

Ion pairs are formed between two species with opposite charges that are not totally separated from each other in solution.[1,2] They are almost always present in charged surfaces and interfaces, and therefore, they are widespread in several fields of science.[3−5] Chemical reactivity and photoreactivity of molecules are related not only to the formation of ion pairs but also to the presence or absence of solvent molecules between the two species that form it.[4−8] In areas such as medicinal chemistry and new materials, ion pairs play important roles. The partition of drugs in membranes, its pharmacokinetics distribution, and consequently its efficacy are dependent on the presence of ion pairs.[9] Spatial control and novel properties are observed in nanostructured thin films, which are frequently constructed on the basis of ion pair formation.[9,10]

In terms of biochemistry and biology, ion pairs are important counterparts of the structure and functionality of membranes, proteins, and DNA. Some fundamental questions in biochemistry, i.e., the actual charge of a DNA molecule in aqueous solution, how ions such as calcium affect the structure and dynamics of membranes, and the role of ion pairs in keeping the protein native conformation, have not been completely answered.[11−13]

The formation of ion pairs is related to several forces that affect the chemical potential of the solvated free species and the ion pairs themselves.[4] Small soluble charged species usually form ion pairs in low dielectric constant solvents. In polar solvents, such as water, solvation interactions greatly overcome ion pair interactions.[1,2,4,5]

In surfaces and interfaces there is a competition between the entropically driven counterion dissociation and the enthalpic changes due to ion−ion and ion−induced dipole interactions. Depending on the charge density of the surface and the strength of the ion−surface interaction, ionic condensation may be extremely large.[14] However, the development of accurate theoretical models able to predict ion binding in surfaces has proven to be a difficult task. Surfaces and interfaces are complex regions where, in a spatial range of a few angstroms, there are strong differences in solvation forces and dielectric constants, which affect the interaction of ions and consequently the dynamics and structure of the surface.[3,14−17]

An interesting example of the importance of ion condensation in shaping superstructures of molecules is the sphere-to-rod

* To whom correspondence should be addressed. E-mail: baptista@iq.usp.br. Phone: +55 11 30913815 221. Fax: +55 11 3815-5579.

† IQ-USP.

‡ IF-USP.

(1) Taft, R. W.; Abraham, M. H.; Doherty, R. M.; Kamlet, M. J. *J. Am. Chem. Soc.* **1985**, *107*, 3105.

(2) Szpakowska M.; Czaplicka I.; Nagy O. B. *Biophys. Chem.* **2006**, *120*, 148.

(3) Yamamoto, R.; Matsumoto, H.; Tanioka, A. *J. Phys. Chem. B* **2003**, *107*, 10506.

(4) Nagy, P. I.; Takacs-Novak, K. *J. Am. Chem. Soc.* **2000**, *122*, 6583.

(5) Taguchi, S.; Takayoshi, K.; Yotsu, Y.; Kasahara, I. *Analyst* **1996**, *121*, 1621.

(6) de Borba, E. B.; Amaral, C. L. C.; Politi, M. J.; Villalobos, R.; Baptista, M. S. *Langmuir* **2000**, *16*, 5900.

(7) Chatterjee, S.; Davis, P. D.; Gottschalk, P.; Kurz, M. E.; Sauerwein, B.; Yang, X. Q.; Schuster, G. B. *J. Am. Chem. Soc.* **1990**, *112*, 6329.

(8) Yang, X. Q.; Zaitsev, A.; Sauerwein, B.; Murphy, S.; Schuster, G. B. *J. Am. Chem. Soc.* **1992**, *114*, 793.

(9) Kaschak, D. M.; Lean, J. T.; Waraksa, C. C.; Saupe, G. B.; Usami, H.; Mallouk, T. E. *J. Am. Chem. Soc.* **1999**, *121*, 3435.

(10) Zucolotto, V.; Gattas-Asfura, K. M.; Tumolo, T.; Perinotto, A. C.; Antunes, P. A.; Constantino, C. J. L.; Baptista, M. S.; Leblanc, R. M.; Oliveira, O. N. *Appl. Surf. Sci.* **2005**, *246*, 397.

(11) Rodenbeck, M.; Muller, M.; Huster, D.; Arnold, K. *Biophys. Chem.* **2001**, *90*, 255.

(12) Arnold, K. *Structure and Dynamics of Membranes: Generic and Specific Interactions*; Elsevier: Amsterdam, 1995; Vol. 1B.

(13) Dias, L. G.; Florenzano, F. H.; Reed, W. F.; Baptista, M. S.; Souza, S. M. B.; Alvarez, E. B.; Chaimovich, H.; Cuccovia, I. M.; Amaral, C. L. C.; Brasil, C. R.; Romsted, L. S.; Politi, M. J. *Langmuir* **2002**, *18*, 319.

(14) Romsted, L. S. In *Reactions and Synthesis in Surfactant Systems*; Texter, J., Ed.; Marcel Dekker: New York, 2001; p 265.

(15) Buurma, N. J.; Serena, P.; Blandamer, M. J.; Engberts, J. *J. Org. Chem.* **2004**, *69*, 3899.

(16) Faeder, J.; Ladanyi, B. M. *J. Phys. Chem. B* **2000**, *104*, 1033.

(17) Mafe, S.; Ramirez, P.; Tanioka, A.; Pellicer, J. *J. Phys. Chem. B* **1997**, *101*, 1851.

10.1021/la061117p CCC: $33.50
Published on Web 09/15/2006

transition in cationic micelles. This transition has a remarkable dependence on the type of surfactant counterion.[18−20] The stabilization of rod-type micellar aggregates has been related to the formation of ion pairs between the headgroup and the counterions, which is accompanied by a decrease in the surface hydration.[18−20]

Although other classifications have already been presented, it is possible to classify the ion pairs into two kinds: contact ion pairs (CIPs) and solvent-separated ion pairs (SSIPs).[1−4,21−23] The difference between them is that the SSIPs have at least one solvent molecule between the ionic counterparts, whereas contact ion pairs do not. Several methods have been used to characterize ion pairs, including Raman, fluorescence, NMR, and UV−vis spectroscopy and ionic conductivity.[1−4,21] However, distinguishing the ion pairs from their separated counterparts as well as characterizing the ion pair species as CIPs and SSIPs is not trivial. New theoretical models have made important contributions to the understanding of ion pairs in surfaces.[22,23] Nevertheless, the experimental characterization of the type of ion pairs present in interfaces and membrane mimetic systems is still elusive.[3,17,19]

Micelles and reverse micelles are supramolecular aggregates that have been widely used to mimic the properties of surfaces and membranes.[6,7,22] When one is interested in studying the water structure or solvation properties close to the interface, reverse micelles are especially useful. By varying the water to surfactant molar ratio (w_0 = [water]/[surfactant]), they provide a well-controlled system to study surface properties, including the curvature, amount of interfacial water, and charge density.[6,16,22]

In this work we characterized the formation and the type of ion pairs between crystal violet (CV) and sodium bis(2-ethylhexyl)sulfosuccinate (AOT) in isotropic solutions and in the negatively charged surfaces of AOT reverse micelles (RMs). The effect of CV on the structure of the AOT RM was studied by small-angle X-ray scattering (SAXS). The CV localization in the AOT RM was characterized by using ^{1}H and ^{13}C NMR spectroscopy. The ion pair formation in isotropic solvents as well as in AOT RMs and the effect of the amount of water in the type of ion pair formed between AOT and CV were studied by UV−vis spectroscopy. Furthermore, quantum chemical calculations were performed to help the rationalization of the results obtained.

The reason for the choice of CV is two-fold. The formation of CV ion pairs (CIPs and SSIPs) affects its internal structural symmetry and its electronic energy levels, and therefore, it can be easily visualized and quantified by UV−vis spectroscopy.[24] Consequently, it was possible to visualize the effect that the amount of interfacial water has on the formation of CIPs and SSIPs. The second reason for the choice of CV is that it is being considered as a drug for use in photodynamic therapy.[25−27] Its mechanism of action is related to targeting of the mitochondrial internal membrane and the photoactivated formation of radicals and singlet oxygen.[25−27] These photoactivated chemical reactions of CV may be affected by the formation of ion pairs.[6−8,28]

Experimental Section

Materials. CV was recrystallized from methanol. AOT purification followed previously published procedures.[29] Briefly, it was purified through reflux in methanolic solution with activated coal. The mixture was filtered and the solvent extracted by vacuum. AOT was dried and stored in vacuum over phosphorus pentoxide and calcium chloride. The limiting amounts of water solubilized by AOT were measured by Karl Fischer titration.[30] In a 0.2 mol L^{-1} AOT solution in isooctane, the water content was determined to be 1×10^{-3} mol L^{-1}. Chloroform was refluxed and distilled over P_2O_5. The other solvents used were spectroscopy grade from Aldrich. Demineralized water was used throughout (18 MΩ, Milli-Q, Millipore).

Sample Preparation. The AOT RM was prepared in isooctane. The solutions were translucent and were prepared and used on the same day. A specific volume of water was added in the solution to prepare the RM with a defined molar ratio of water to surfactant (w_0). The CV concentration was determined on the basis of the value of its molar extinction coefficient (0.95×10^5 mol^{-1} L cm^{-1}) in water.[24−26] To obtain an RM solution with a specific CV concentration, a CV stock solution was prepared in water and a specific volume of this solution was added to the RM. For the experiments whose w_0 was altered, aliquots of CV aqueous solution, which had the same CV concentration as in the RM, were added to the micelle solution, so that w_0 could be altered without changing the CV concentration. All solutions were agitated for 5 min to achieve a homogeneous ternary mixture.

UV−Vis Spectrophotometry. The absorbance spectra were recorded using a Shimadzu UV-2401PC UV−vis spectrophotometer interfaced to a microcomputer. All experiments were made at T = 25 °C. The ion pair equilibrium constants were obtained by calculating the concentration of associated ([CV−AOT]) and free ([CV]) CV by the changes in the UV−vis spectra.[24] The plot of [CV−AOT]/[CV] as a function of AOT concentration allows the calculation of K_{ASSOC}. Next, K_{ASSOC} as a function of w_0 was obtained by calculating the values of CV−AOT and CV concentrations at each w_0 value. In these experiments the AOT concentration was kept constant. ΔG values were calculated directly from K_{ASSOC} (eq 3).

$$\mathrm{CV} + \mathrm{AOT} \underset{K_{ASSOC}}{\rightleftharpoons} \mathrm{CV{-}AOT} \tag{1}$$

$$K_{ASSOC} = \frac{[\mathrm{CV{-}AOT}]}{[\mathrm{CV}][\mathrm{AOT}]} \quad \text{so} \quad K_{ASSOC}[\mathrm{AOT}] = \frac{[\mathrm{CV{-}AOT}]}{[\mathrm{CV}]} \tag{2}$$

$$\Delta G = -RT \ln K_{ASSOC} \tag{3}$$

NMR Spectroscopy. Samples in the presence or absence of CV at low and high w_0 were prepared as described above, with the exception that deuterated water was used to change w_0. The organic phase used was also isooctane. The peak identification of the ^{1}H and ^{13}C NMR spectra was based on the previously published AOT spectra.[31,32] NMR spectra were obtained with a Bruker DRX 500 spectrometer operating at 500 MHz.

SAXS. Small-angle X-ray scattering curves were obtained by using a small-angle setup coupled to a Rigaku-Denki (18 kW) rotating anode with a line beam transmission geometry and X-ray wavelength Cu Kα radiation (graphite monochromator, λ = 1.5418 Å). The scattering intensity was corrected by the solvent contribution, taking into account the attenuation of the sample.

(18) Kreke, P. J.; Magid, L. J.; Gee, J. C. *Langmuir* **1996**, *12*, 699.
(19) Geng, Y.; Romsted, L. S.; Froehner, S.; Zanette, D.; Magid, L. J.; Cuccovia, I. M.; Chaimovich, H. *Langmuir* **2005**, *21*, 562.
(20) Geng, Y.; Romsted, L. S.; Menger, F. M. *J. Am. Chem. Soc.* **2006**, *128*, 492.
(21) Pochapsky, T. C.; Stone, P. M.; Pochapsky, S. S. *J. Am. Chem. Soc.* **1991**, *113*, 1460.
(22) Faeder, J.; Albert, M. V.; Ladanyi, B. M. *Langmuir* **2003**, *19*, 2514.
(23) Chorny, I.; Dill, K. A.; Jacobson, M. P. *J. Phys. Chem. B* **2005**, *109*, 24056.
(24) Oliveira, C. S.; Branco, K. P.; Baptista, M. S.; Indig, G. L. *Spectrochim. Acta, Part A* **2002**, *58*, 2971.
(25) Baptista, M. S.; Indig, G. L. *Chem. Commun.* **1997**, *18*, 1791.
(26) Baptista, M. S.; Indig, G. L. *J. Phys. Chem. B* **1998**, *102*, 4678.
(27) Indig, G. L.; Anderson, G. S.; Nichols, M. G.; Bartlett, J. A.; Mellon, W. S.; Sieber, F. *J. Pharm. Sci.* **2000**, *89*, 88.
(28) Tolmachov, A. I.; Zaitsev, A. K.; Koska, N.; Schuster, G. B. *J. Photochem. Photobiol., A* **1994**, *77*, 237.
(29) El Seoud, O. A.; Fendler, J. H. *J. Chem. Soc., Faraday Trans.* **1975**, *3*, 452.
(30) Vogel, A. *Vogel's Textbook of Quantitative Inorganic Analysis*; Longman Scientific & Technical: London, 1989.
(31) Lissi, E. A.; Encinas, M. V.; Lemp, E.; Rubio, M. A. *Chem. Rev.* **1993**, *93*, 699.
(32) Yoshino, A.; Sugiyama, N.; Okabayashi, H.; Taga, K.; Yoshida, T.; Kamo, O. *Colloids Surf.* **1992**, *67*, 67.

The scattering intensity from a set of monodisperse particles with electron density ρ randomly distributed in a medium of electron density ρ_0 is given by[33−35]

$$I(q) = \gamma n_p(\Delta\rho)^2 V^2 P(q) S(q) \quad (4)$$

where $q = (4\pi \sin\theta)/\lambda$ is the scattering vector and 2θ the scattering angle, γ is a factor related to the instrumental effects, n_p corresponds to the particle number density, $\Delta\rho = \rho - \rho_0$ is the electron density contrast between the scattering particle and the medium, V is the scattering particle volume, $P(q)$ is the normalized particle form factor ($P(0) = 1$), and $S(q)$ is the interparticle interference function. For systems with small polidispersity (<20%), the deviation corresponds to a diffuse background scattering[36] that is accounted for in the data treatment.

In the case of noninteracting systems, $S(q) \rightarrow 1$, a Fourier transform connects $I(q)$ to the pair distance distribution function, $p(r)$, the probability of finding a pair of small elements at a distance r within the entire volume of the scattering particle as:[33−35]

$$p(r) = (1/2\pi^2)\int_0^\infty I(q)\, qr \sin(qr)\, dq \quad (5)$$

This function provides information about the shape of the scattering particle as well as its maximum dimension, D_{max}, accounted for at a certain r value where $p(r)$ goes to zero. For spheres, $p(r)$ is symmetrical with a maximum value at $r = R$, the particle radius ($D_{max} = 2R$). Moreover, the particle radius of gyration, R_g, can be evaluated through:[35−38]

$$R_g^2 = \frac{\int_0^{D_{max}} p(r)\, r^2\, dr}{2\int_0^{D_{max}} p(r)\, dr} \quad (6)$$

In particular for spheres, $R^2 = (5/3)R_g^2$. In this work, we make use of the indirect Fourier transform process[37] developed by O. Glatter et al. by means of a software package (Generalized GIFT[38]) to calculate $p(r)$ from the SAXS curves. Such a procedure takes into account the smearing effect caused by the incident X-ray line beam (negligible width).

Quantum Chemical Calculations. Molecular geometries were calculated by means of the semiempirical PM3 method.[39] At first we calculated the optimized structure of a free CV, constrained to a D_3 symmetry. Next, we calculated the equilibrium location of a counterion, namely, chloride or AOT, initially positioned 4 Å above the central carbon in CV. The AOT structure was obtained by means of a conformational search starting from the two enantiomeric forms of AOT, obtained by varying the chiral center at the carbon bonded to the sulfonate group. The lowest energy resulting conformers were selected and the structures compared with that suggested by interpretation of 2-D NMR data.[40] All stationary points were confirmed as minima via vibrational frequency calculations.

The polarized split-valence double-ζ basis set 6-31G(d) was used in calculating magnetic shielding constants σ by the gauge-independent atomic orbital (GIAO) method. NMR ^{13}C and ^{1}H chemical shifts δ were obtained by subtracting the calculated magnetic shielding calculated with reference to tetramethylsilane (TMS).

Because of the high computational expenditure in calculating UV−vis spectral features by high-level correlated ab initio methods, organic compounds were studied by the semiempirical ZINDO-CI method. Furthermore, this method needs no parametrization in excited-state calculations and is applicable for the main groups of elements of the periodic table. The geometries of the CV^+Cl^- and CV^+AOT^- ion pairs were separately optimized at the PM3 level, the chloride and AOT were deleted, and the resulting CV was submitted to ZINDO-CI molecular orbital calculation. All calculations were performed using the Gaussian 03 suite of programs on an HP cluster of AlphaServers at the Laboratório de Computação Científica Avançada (LCCA), Universidade de São Paulo.[41] Three-dimensional chemical structures were obtained using ArgusLab 4.0.1 software.[42]

Results

Effect of CV on the AOT RM Structure. There have been several reports in the literature showing how additives dissolved in the water core of the AOT RM could modify its structure.[36,43] To study the effect of the CV on the structure of the AOT RM, SAXS experiments were carried out with samples composed of AOT/isooctane/water at $w_0 = 0.9$, 10.6, and 20.0 in the absence and presence of increasing CV concentrations ([CV] = 4.5, 22, and 150 μmol L^{-1}).

SAXS data and analysis of AOT RMs in the presence of 150 μmol L^{-1} CV at w_0 values of 0.9 and 10.6 (identical for the other CV concentrations) are shown in Figure 1. As can be observed, the scattering is typical of spherical droplets with core radii (R_c) of 11.6 ± 0.6 and 34.0 ± 1.0 Å at $w_0 = 0.9$ (Figure 1A) and 10.6 (Figure 1B), respectively. Such values were evaluated from the maximum dimension values D_{max} (associated with the sphere diameters) and radii of gyration R_g (eq 6) obtained from the pair distance distribution function $p(r)$ curves (insets in Figure 1). These SAXS curves and, hence, the parameters obtained from them are identical to those found in AOT RMs without CV (data not shown) and are equivalent to other published data.[36,43] Similar results were observed for $w_0 = 20$; i.e., the SAXS curves were identical in the presence and absence of CV. Therefore, the addition of CV to RMs does not promote any significant change in their size and shape, and the data presented below can be analyzed in such terms.

Localization of CV in AOT RMs by NMR. NMR spectroscopy has become an important tool to characterize the normal and RM structure and dynamics.[44−46] The structure and state of the water in AOT RMs were investigated by ^{1}H, ^{23}Na, and ^{13}C NMR.[47,48] The solubilization of dyes[49,50] and ions[46] and their

(33) Guinier, A.; Fournet, G. *Small Angle Scattering of X-rays*; Wiley: New York, 1955.
(34) Kotlarchyk, M.; Chen, S. H. *J. Chem. Phys.* **1983**, *79*, 2461.
(35) Glatter, O. *Small Angle X-ray Scattering*; Academic Press: London, 1982.
(36) Itri, R.; Amaral, C. L. C.; Politi, M. J. *J. Chem. Phys.* **1999**, *111*, 7668.
(37) Glatter, O. *J. Appl. Crystallogr.* **1977**, *12*, 166.
(38) Weyerich, B.; Brunner-Popela, J.; Glatter, O. *J. Appl. Crystallogr.* **1999**, *32*, 197.
(39) Del Nero, J.; Galembeck, A.; Silva, S. B. C.; Silva, J. A. P. *Mater. Res.* **2003**, *6*, 335.
(40) Yoshino, A.; Okabayashi, H.; Yoshida, T.; Kushida, K. *J. Phys. Chem.* **1996**, *100*, 9592.
(41) Frisch, M. J.; Trucks, G. W.; Schlegel, H. B.; Scuseria, G. E.; Robb, M. A.; Cheeseman, J. R.; Montgomery, J., J. A.; Vreven, T.; Kudin, K. N.; Burant, J. C.; Millam, J. M.; Iyengar, S. S.; Tomasi, J.; Barone, V.; Mennucci, B.; Cossi, M.; Scalmani, G.; Rega, N.; Petersson, G. A.; Nakatsuji, H.; Hada, M.; Ehara, M.; Toyota, K.; Fukuda, R.; Hasegawa, J.; Ishida, M.; Nakajima, T.; Honda, Y.; Kitao, O.; Nakai, H.; Klene, M.; Li, X.; Knox, J. E.; Hratchian, H. P.; Cross, J. B.; Bakken, V.; Adamo, C.; Jaramillo, J.; Gomperts, R.; Stratmann, R. E.; Yazyev, O.; Austin, A. J.; Cammi, R.; Pomelli, C.; Ochterski, J. W.; Ayala, P. Y.; Morokuma, K.; Voth, G. A.; Salvador, P.; Dannenberg, J. J.; Zakrzewski, V. G.; Dapprich, S.; Daniels, A. D.; Strain, M. C.; Farkas, O.; Malick, D. K.; Rabuck, A. D.; Raghavachari, K.; Foresman, J. B.; Ortiz, J. V.; Cui, Q.; Baboul, A. G.; Clifford, S.; Cioslowski, J.; Stefanov, B. B.; Liu, G.; Liashenko, A.; Piskorz, P.; Komaromi, I.; Martin, R. L.; Fox, D. J.; Keith, T.; Al-Laham, M. A.; Peng, C. Y.; Nanayakkara, A.; Challacombe, M.; Gill, P. M. W.; Johnson, B.; Chen, W.; Wong, M. W.; Gonzalez, C.; Pople, J. A. *Gaussian 03*; Gaussian, Inc.: Wallingford, CT, 2004.
(42) Thompson, M. A. *ArgusLab*, 4.0.1 ed.; Planaria Software LLC: Seattle, 2005.
(43) Filankembo, A.; André, P.; Lisiecki, I.; Petit, C.; Gulik-Krzywicki, T.; Ninham, B. W.; Pileni, M. P. *Colloids Surf., A* **2000**, *174*, 221.
(44) Chachaty, C. *Prog. Nucl. Magn. Reson. Spectrosc.* **1987**, *19*, 183.
(45) Tiddy, G. J. T. *Phys. Rep.* **1980**, *57*, 2.
(46) Nagy, J. B.; Bodartravet, I.; Derouane, E. G.; Gourgue, A.; Verfaillie, J. P. *Colloids Surf.* **1989**, *36*, 229.
(47) Wong, M.; Thomas, J. K.; Nowak, T. *J. Am. Chem. Soc.* **1977**, *99*, 4730.
(48) El Seoud, O. A.; El Seoud, M. I.; Mickiewicz, J. A. *J. Colloid Interface Sci.* **1994**, *163*, 87.
(49) Shah, S. S.; Windsor, M. W. *Chem. Phys. Lett.* **1982**, *92*, 33.
(50) Huang, X. R.; Zhang, W. J.; Zhang, Z. Y.; Xu, G. Y.; Li, C. P. *Spectrochim. Acta, Part A* **1998**, *54*, 617.

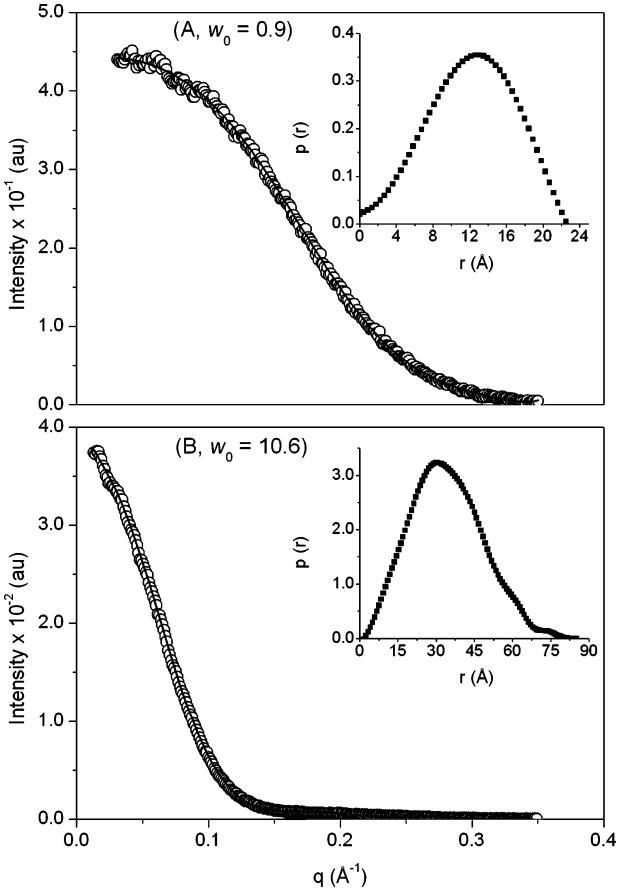

Figure 1. (A) Small-angle X-ray scattering data (—) of AOT/isooctane/water at (A) $w_0 = 0.92$ and (B) 10.65 in the presence of 150 μmol L^{-1} CV. The SAXS curves of RMs in the absence of CV are identical and hence not shown here. The insets display the corresponding distance distribution functions, $p(r)$.

interactions with micellar structures were also studied by this technique. The effect of the addition of CV molecules on the ^{1}H and ^{13}C chemical shifts of the AOT molecule can be analyzed considering three effects: (i) ring shift effect, i.e., shielding of aromatic rings in the surroundings protons and carbons, (ii) effect of the charge of CV, (iii) changes in AOT headgroup solvation related to the presence of CV in the interface.[51−53]

Shown in Table 1 are the absolute ($\Delta\nu$) and the relative ($\Delta\nu/\Delta\nu_0$; see below) variations in ^{1}H chemical shifts of AOT RMs observed upon adding CV (see Scheme 1 for the AOT proton/carbon designation). The absolute variation in the chemical shift ($\Delta\nu$) is defined as the chemical shift of a specific AOT proton or carbon in the presence of CV subtracted from the chemical shift of the same proton obtained in the absence of CV. The results show that all protons have significant $\Delta\nu$ values (Table 1 and Scheme 1A). To visualize protons that presented the largest variations, $\Delta\nu$ values were divided by the $\Delta\nu$ experienced by the terminal methylene group ($\Delta\nu_0$), i.e., $\Delta\nu/\Delta\nu_0$. Note that, at low w_0, protons grouped as D have relative variations as high as 500% ($\Delta\nu/\Delta\nu_0 = 5.3$), protons F around 50−60% ($\Delta\nu/\Delta\nu_0 = 1.6$), and protons C around 30% ($\Delta\nu/\Delta\nu_0 = 1.3$) (Table 1). The protons that presented the largest variations (D and F, Table 1) are the protons nearest to the negatively charged sulfosuccinate group (SG) of AOT. The protons grouped as C are ca. 6 Å from the carbon bonded to the sulfonate group. This distance is equivalent to the distance of the amine−aromatic ring of CV from its central carbon, suggesting that the central positively charged group of CV is on average located in close proximity to SG, and some of its aromatic rings and the amine groups

Table 1. Absolute ($\Delta\nu_{NMR}$) and Relative ($\Delta\nu/\nu_0$) Change of the Chemical Shift of ^{1}H NMR of the AOT Reverse Micelles at w_0 = 0.1 and 20.0 in the Absence and Presence of CV

	$w_0 = 0.1$			$w_0 = 20.0$	
a, *b*	$\Delta\nu_{NMR}$[c] (Hz)	$\Delta\nu/\nu_0$[d]	*a*, *b*	$\Delta\nu_{NMR}$[c] (Hz)	$\Delta\nu/\nu_0$[c]
A (1.1)	3.9	1.0	A (1.0)	−58.1	1.0
	4.0			−51.4	
	4.0				
B (1.3)	3.9	1.0	B (1.2)	−52.7	0.9
	3.9	1.0			
	3.9	1.0			
C (3.5)	5.3	1.3	C (3.3)	−58.8	1.0
	5.3	1.3		−75.9	1.3
				−73.4	1.3
				−69.4	1.2
				−64.1	1.1
				−69.6	1.2
D (4.2)	12.4	3.2	D (4.1)	−85.8	1.5
	12.1	3.1		−89.0	1.5
	20.7	5.3		−85.9	1.5
	20.8	5.3			
E (4.4)	2.2	0.6	E (4.3)	−60.3	1.0
	2.4	0.6		−60.4	1.0
	2.7	0.7		−60.3	1.0
				−63.5	1.1
				−64.8	1.1
				−70.5	1.2
F (4.6)	6.1	1.6	F (4.4)	−59.1	1.0
	6.5	1.7		−59.0	1.0
	6.1	1.6		−59.0	1.0
	6.1	1.6		−59.0	1.0

[a] [AOT] = 0.4 mol L^{-1}, and [CV] = 4.0 mmol L^{-1}. [b] The letters correspond to the protons that present variations in ν upon adding CV, and the values in parentheses represent the actual chemical shift obtained (ppm). See Scheme 1A for the ^{1}H NMR designation. [c] $\Delta\nu_{NMR}$ = relative variation of the chemical shift, with and without CV at $w_0 = 0.1$ and 20, in Hertz. [d] $\Delta\nu/\nu_0$ = percentage of the variation; ν_0 is the chemical shift of the terminal methylene group (A).

Scheme 1. Chemical Structure of the AOT Molecule[a]

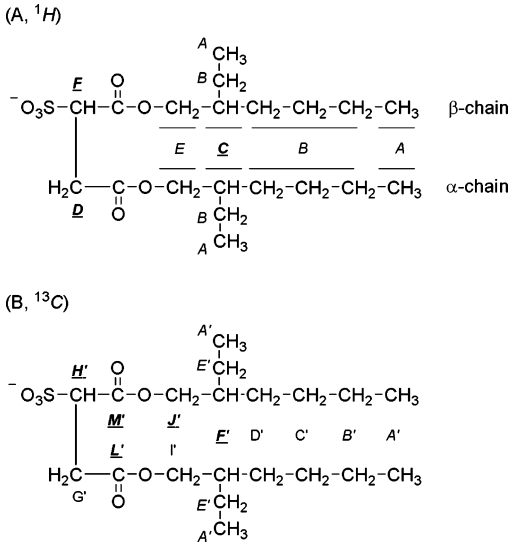

[a] The letters correspond to the peaks obtained in the spectra of (A) ^{1}H and (B) ^{13}C NMR. Protons and carbons that experienced the highest shift upon addition of CV are in bold and underlined.

(51) Günther, H. *NMR Spectroscopy: Basic Principles, Concepts, and Applications in Chemistry*, 2nd ed.; Wiley: New York, 1995.
(52) Sohár, P. *Nuclear Magnetic Resonance Spectroscopy*; CRC Press: Boca Raton, FL, 1984; Vol. 1.
(53) Silverstein, R. M.; Bassier, G. C.; Morrill, T. C. *Spectrometric Identification of Organic Compounds*; Wiley: New York, 1991.

Table 2. Absolute ($\Delta\nu_{NMR}$) and Relative ($\Delta\nu/\nu_0$) Change of the Chemical Shift of ^{13}C NMR of the AOT Reverse Micelles at $w_0 = 0.1$ and 20 in the Absence and Presence of CV

$w_0 = 0.1$			$w_0 = 20.0$		
a, *b*	$\Delta\nu_{NMR}$[c] (Hz)	$\Delta\nu/\nu_0$[d]	*a*, *b*	$\Delta\nu_{NMR}$[c] (Hz)	$\Delta\nu/\nu_0$[d]
A′ (11.2)	3.8	1.0	A′ (10.6)	144.7	1.0
	3.1				
B′ (14.3)	1.6	0.4	B′ (13.9)	146.3	1.0
	2.7	0.7		147.6	1.0
C′ (23.4)	1.1	0.3	C′ (23.0)	144.1	1.0
D′ (23.8)	0.6	0.1	D′ (23.5)	146.7	1.0
	0.5	0.1		146.5	1.0
	0.5	0.1		142.5	1.0
E′ (29.4)	1.9	0.5	E′ (28.9)	147.8	1.0
	0.5	0.1			
F′ (33.5)	11.8	3.2	F′ (33.3)	156.0	1.1
G′ (38.2)	2.4	0.6	G′ (38.6)	145.6	1.0
	2.8	0.8		144.4	1.0
	0.6	0.1			
H′ (61.7)	9.8	2.6	H′ (61.7)	152.1	1.1
I′ (67.2)	2.2	0.6	I′ (67.2)	147.2	1.0
				147.8	
J′ (68.6)	−8.8	−2.4	J′ (68.3)	139.7	1.0
				139.8	
L′ (169.9)	−17.5	−4.7	L′ (168.8)	131.5	1.0
M′ (171.7)	−5.5	−1.5	M′ (171.4)	148.0	0.9

[a] [AOT] = 0.4 mol L^{-1}, and [CV] = 4.0 mmol L^{-1}. [a] The letters correspond to the carbons that present variations in *n* upon adding CV, and the values in parentheses represent the actual chemical shift obtained (ppm). See Scheme 1B for the ^{13}C NMR designation. [c] $\Delta\nu_{NMR}$ = relative variation of the chemical shift, with and without CV at $w_0 = 0.14$ and 20, in Hertz. [d] $\Delta\nu/\nu_0$ = percentage of the variation. ν_0 is the chemical shift of the terminal methylene group (A).

localize in the AOT side of the interface, interacting with the protons C and carbons F′ (Scheme 1).

At $w_0 = 20$, there are large shifts to high field upon addition of CV ($\Delta\nu$ is negative). The reason the chemical shift is toward high field at $w_0 = 20$ is probably related to the release of water molecules from the RM interface; i.e., water interacts strongly through hydrogen bonds with the SG of AOT, and breaking the hydrogen bond network results in high-field shifts.[54,55] The values of $\Delta\nu/\Delta\nu_0$ are smaller compared to those observed at low w_0 values (Table 1). However, at this w_0 it is also possible to observe that protons D and C present the largest $\Delta\nu/\Delta\nu_0$, suggesting that although the magnitude of the interactions between the CV and AOT is smaller at this w_0, the CV localization is also in close proximity to SG.

Similar results were observed in the ^{13}C NMR experiments (Table 2). Note that, by adding CV, $\Delta\nu$ is either negative or positive (variations toward high or low field, respectively). The understanding of the sign of $\Delta\nu$ is difficult because it may be caused by interactions of CV with the AOT carbon atoms or changes in AOT solvation. By looking at the magnitude of $\Delta\nu/\Delta\nu_0$, it is possible to observe that the largest variations are in carbons F′, H′, J′, L′, and M′. As can be observed in Scheme 1, these carbons are also located in close proximity or are ca. 6 Å from the SG group, in agreement with the ^1H NMR results. The higher effect observed in the β-chain carbons F′, J′, and M′ when compared with the α-chain carbons F′, I′, and L′ can be explained by the fact that the α-chain is more restricted (i.e., rigid) than the β-chain, being responsible for the thickness of the hydrophobic core.[40] Thus, it is likely that the β-chain takes adequate

Scheme 2. Newman Projection of the Most Stabilized Rotational Conformer for AOT in the Reverse Micellar State[46]

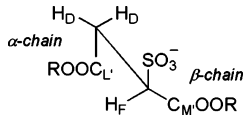

conformations to fill the grooves among the AOT RMs, resulting in higher interaction with CV.

At $w_0 = 20$ the magnitude of the variations observed is lower than at $w_0 = 0.1$. However, the carbons that exhibit the largest variations (F′ and H′) identify the same interfacial region for the CV localization. Therefore, ^1H and ^{13}C NMR experiments show that CV is located in the interface of AOT RMs in close proximity to the SG group at low and high w_0 values.

The effect of CV on the ^1H and ^{13}C chemical shifts of AOT was also investigated using quantum chemical calculations. Since AOT has a significant size, several conformational degrees of freedom, and three asymmetric carbon atoms (H′, αF′, and βF′, resulting in eight possible diastereoisomers), a minimum theoretical model is proposed to reduce the computational costs, as follows. The configuration of the chiral centers at carbons αF′ and βF′ where both set as *R* and the two resulting enantiomeric forms of AOT, obtained by varying the configuration of the asymmetric carbon H′, where submitted to a full conformational search (molecular mechanics). The lowest energy conformers were selected and the structures compared with that suggested by interpretation of $^{13}CT_1$ NMR, ^1H NMR, NOESY, and ROESY data, i.e., the best agreement with the following conditions: the preferentially stabilized rotational isomer in the RM (Scheme 2), showing the proximity of protons C of the α and β chains and dipole−dipole contact with $^1H\alpha C$ and $^1H\beta B$, $^1H\beta C$ and $^1H\alpha B$, and $^1H\beta C$ and $^1H\alpha A$ (Scheme 1).[40]

The resulting single isomer was optimized at the PM3 level, and the magnetic shielding constants were calculated using the GIAO method with the HF/6-31G(d) basis set. The obtained chemical shifts (with reference to TMS) were compared with those presented in Tables 1 (^1H) and 2 (^{13}C), resulting in good linear correlation coefficients ($\delta^H = 0.073 + 1.03\delta^{H,Th}$, $r = 0.95$, and $\delta^C = 0.346 + 0.99\delta^{C,Th}$, $r = 0.99$) (Table 3). Considering that, in these calculations other AOT, solvent, and water molecules are absent, we think that the linear correlation coefficients of 0.95 and 0.99 obtained respectively for ^1H NMR and ^{13}C NMR shifts are good. One must also consider that AOT has 37 hydrogen atoms and only 20 carbon atoms; therefore, a better correlation between experimental and theoretical data is expected for carbon than for hydrogen shifts.

The obtained AOT structure was put together with a CV constrained to a propeller-like structure (D_3 symmetry), with the negatively charged oxygen of SG being 4 Å away from the central carbon of CV. The resulting ion pair was submitted to geometry optimization at the semiempirical PM3 level. Next, to obtain the lowest energy rotational conformer, the CV counterpart was submitted to a potential energy scan for the rotation of the dihedral formed by $C^{10}{}_{CV}-C^{2}{}_{CV}-O_{AOT}-S_{AOT}$ along the *x* axis. The relative energies of 11 rotamers and the optimized structure of the lowest energy one are depicted in parts A and B of Figure 2, respectively. One should notice in Figure 2B that the aromatic ring is positioned along the α and β chains of AOT, close to the protons C and carbons F′. Although this calculation has been done for a single molecular complex and not for an RM interface, the relative positions of CV and AOT in the stabilized complex are in agreement with the structural hypothesis used to explain the NMR data.

(54) Novaki, L. P.; Correa, N. M.; Silber, J. J.; El Seoud, O. A. *Langmuir* **2000**, *16*, 5573.
(55) El Seoud, O. A.; Correa, N. M.; Novaki, L. P. *Langmuir* **2001**, *17*, 1847.

Table 3. Comparison between Theoretical and Observed Chemical Shifts (δ) for AOT

δ^{H} (ppm)	$\delta^{H,Th}$ [a] (ppm)	^{1}H [b]	δ^{C} (ppm)	$\delta^{C,Th}$ [a] (ppm)	^{13}C [b]
4.60	4.01	F	61.70	58.99	H′
4.20	4.22	D	38.20	32.22	G′
4.40	4.11	E	171.70	176.13	M′
4.40	4.40	E	169.90	171.76	L′
1.30	1.76	B	68.60	55.63	J′
1.07	0.92	A	67.20	59.65	I′
1.30	1.00	B	33.50	32.05	F′
1.30	1.15	B	33.50	33.01	F′
1.30	1.86	B	29.40	27.89	E′
1.30	1.87	B	11.20	9.83	A′
1.07	0.82	A	23.80	25.84	D′
1.30	0.73	B	23.40	25.99	C′
1.30	1.70	B	14.30	18.43	B′
1.30	1.17	B	29.40	17.06	E′
1.07	0.91	A	11.20	8.09	A′
1.07	0.93	A	23.80	26.49	D′
3.50	2.85	C	23.40	30.20	C′
3.50	2.34	C	14.30	24.92	B′
			11.20	16.76	A′
			11.20	18.30	A′
r	0.94945		*r*	0.99123	

[a] GIAO/6-31G(d)/PM3 with reference to TMS (HF/6-31G(d), shielding (^{1}H) 32.5976, (^{13}C) 199.9853). [b] See Scheme 1.

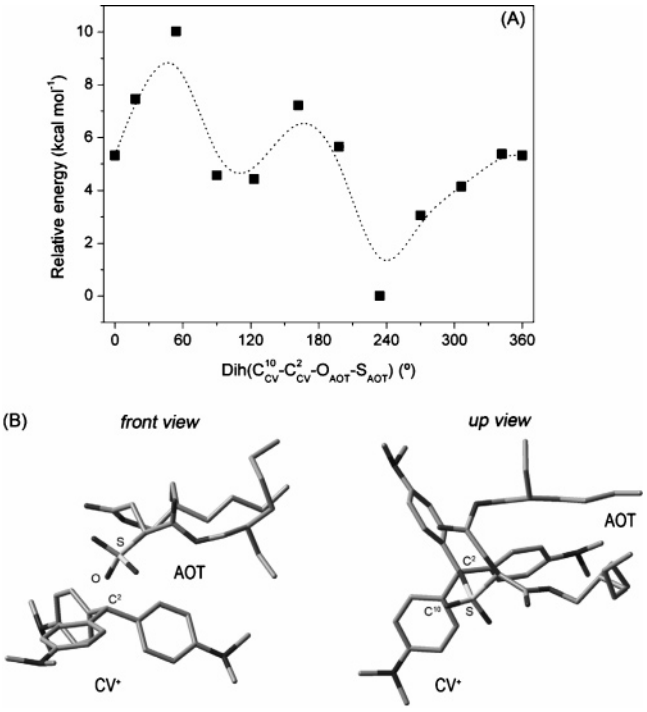

Figure 2. (A) Relative energy of 11 rotamers of the CV−AOT ion pair obtained by varying the $C_{CV}-C_{CV}-O_{AOT}-S_{AOT}$ dihedral angle along the *x* axis, calculated at the PM3 level. (B) Front and up views of the PM3-optimized lowest energy CV−AOT ion pair rotamer. One should notice the position of CV's aromatic ring close to the α and β chains of AOT. All hydrogen atoms were removed for clarity.

CV−AOT Ion Pairs. When the structural symmetry of CV is decreased, especially by the formation of solute−solute interactions (ion pairs or aggregates), its UV−vis spectrum profile changes.[24] We have previously determined that two spectral characteristics are modified: there are a splitting in the absorbance band and a shift in the wavelength of the maximum absorbance (λ_{max}). We have also demonstrated that the only change specifically related to the formation of ion pairs is the red shift

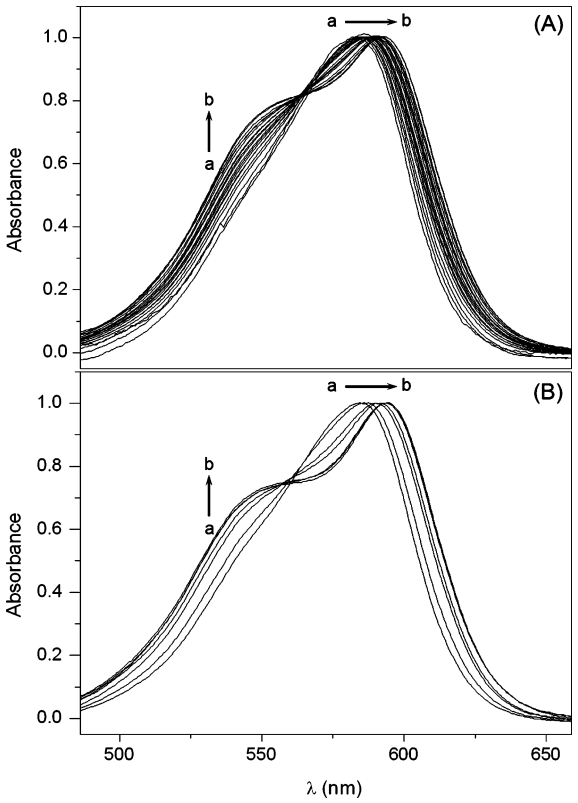

Figure 3. (A) Absorbance spectra of CV at increasing dye concentration in chloroform. From (a) to (b) [CV] (μmol L^{-1}) = 0.3, 0.9, 1.5, 2.1, 3.4, 4.0, 4.9, 6.1, 7.4, 8.6, 13.1, 16.7, 20.4, 37.3, 49.3, 72.8, 108.7, 178.1, 636.3, and 900.1. (B) Absorbance spectra of CV at increasing AOT concentration in chloroform. From (a) to (b) [AOT] = 100 μmol L^{-1}, 1 mmol L^{-1}, 7 mmol L^{-1}, 10 mmol L^{-1}, 50 mmol L^{-1}, 70 mmol L^{-1}, and 100 mmol L^{-1} and [CV] = 1.2 μmol L^{-1}.

in λ_{max}, since a blue shift in λ_{max} takes place upon dimerization (H-type dimers).[24] Usually, ion pair formation is observed in low dielectric constant solvents and aggregation in water.[24] In all experiments of RMs shown here, there is a large concentration excess of AOT in comparison with CV, greatly disfavoring the formation of CV−CV aggregates. Also, the spectral fingerprint of CV dimers, i.e., λ_{max} = 589 nm coupled with large band splitting, was never observed.[24]

Typical spectral changes related to the formation of CV ion pairs in chloroform are shown in Figure 3A. It can be noticed that by increasing the CV concentration there is an increase of absorption at 540 nm and a shift in the maximum wavelength to the red. As has already been mentioned, these changes have been characterized in detail before, being related to the formation of $CV^{+}Cl^{-}$ CIPs.[24] It is possible to estimate the CIP formation constant in chloroform as 1×10^{5} mol^{-1} L. The formation of $CV^{+}Cl^{-}$ CIPs is typical in solvents with low dielectric constants (<5 D), and the equilibrium constant increases with a decrease in the dielectric constant of the medium.[24]

Note that, by increasing the AOT concentration in a chloroform solution with low CV concentration, similar spectral shifts are observed, i.e., appearance of the shoulder at 540 nm and a red shift of the maximum absorbance (Figure 3B). Because at this CV concentration there is an extremely low concentration of $CV^{+}Cl^{-}$ ion pairs, it can be suggested that the ion pair is formed between CV and the AOT molecule. To prove this point, the solubility of CV in isooctane was measured as a function of AOT concentration (Figure 4A). It is possible to observe that the CV solubility increases with an increase in the AOT concentration,

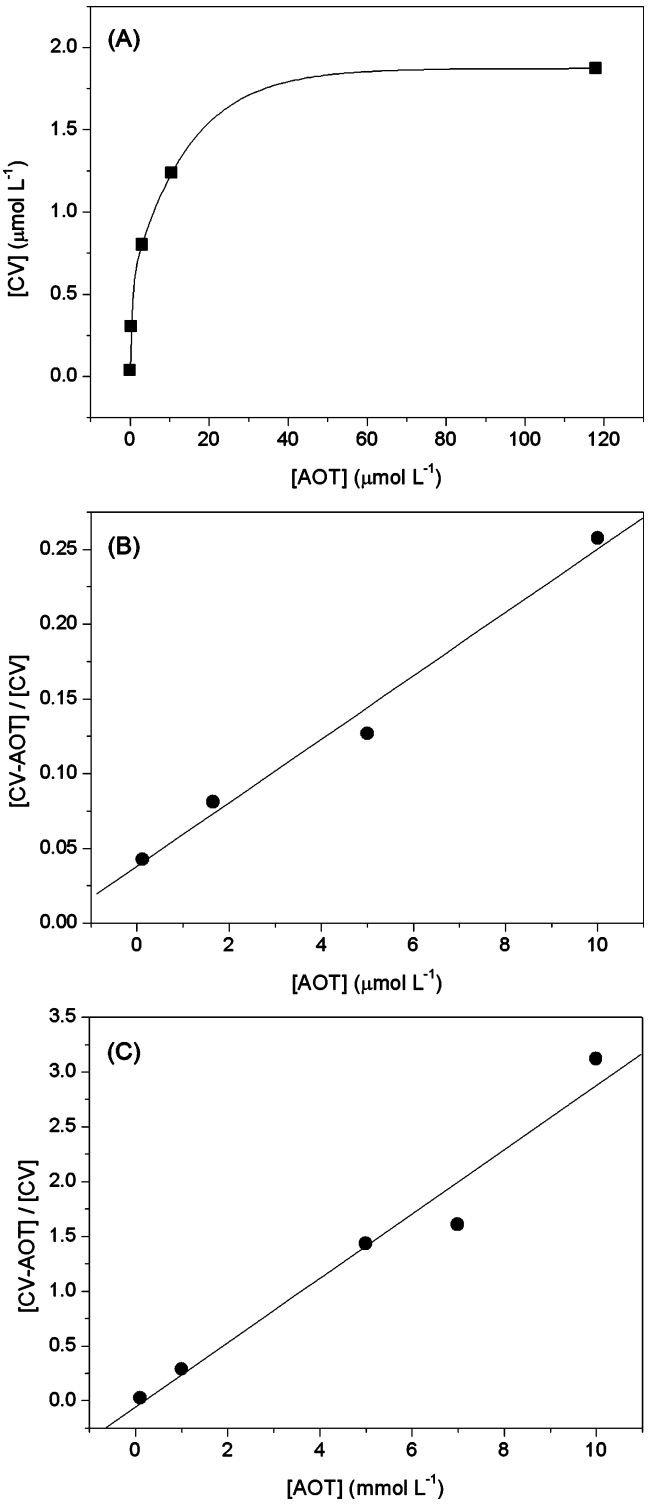

Figure 4. (A) Solubility of CV in isooctane. (B, C) Ratio of associated and free CV molecules in (B) isooctane and (C) chloroform as a function of the AOT concentration.

demonstrating that AOT and CV must form a neutral CIP complex, being soluble in the nonpolar solvent. Using the variations in the absorbance spectra as a function of AOT concentration, the association equilibrium constants (K_{ASSOC}) were calculated (eqs 1 and 2) as 750 mol^{-1} L in chloroform and 2×10^4 mol^{-1} L in isooctane (parts B and C of Figure 4, respectively). As expected, K_{ASSOC} increases as the solvent dielectric constant decreases.

The electronic spectrum of CV changes substantially as a function of w_0 in AOT RMs (Figure 5). The large λ_{max} value

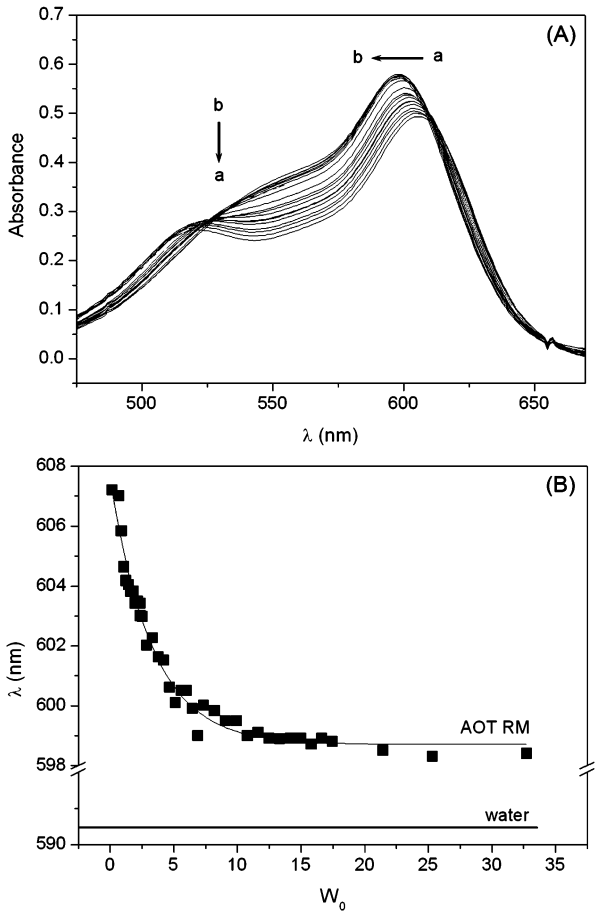

Figure 5. (A) Absorption spectra of CV in AOT RMs at increasing w_0 from (a) to (b): w_0 = 0.7, 1.1, 1.5, 1.6, 2.0, 2.4, 2.5, 3.4, 4.3, 5.2, 6.0, 7.0, 8.2, 10.0, 12.0, 13.4, 14.2, 15.0, 16.7, 21.4, 25.3, and 40.0. (B) λ_{max} of CV in AOT RMs as a function of w_0. [AOT] = 0.2 mol L^{-1}, and [CV] = 5.9 μmol L^{-1}. For comparison λ_{max} in water is also shown. A break in the *y* axis between 591 and 598 nm was inserted for clarity.

($\lambda_{max} \approx 608$ nm) (Figure 5A) observed at low w_0 is the spectroscopic fingerprint characteristic of CV ion pairs.[24] This λ_{max} is larger than the λ_{max} of CV in trichloroethylene, where CV^+Cl^- CIPs are efficiently formed,[24] indicating that CV CIPs are formed in AOT RMs at low w_0 values. Considering that the AOT and chloride concentrations are, respectively, 0.2 and 1×10^{-5} mol L^{-1}, the ion pair in the AOT RM must be mainly formed with the AOT headgroup.

It is also observed in Figure 5 that with an increase in w_0, λ_{max} of CV decreases, i.e., indicating that the initially formed CIP is somehow absent with an increase in w_0. At w_0 values larger than ~20 the values of λ_{max} are constant at ~598 nm (Figure 5B). This λ_{max} is larger than that of free CV in water, which is 590 nm (Figure 5B), and it is lower than the λ_{max} of CV CIPs (typically, $\lambda_{max} \geq 601$ nm). Considering that the water concentration in the interfacial region of the AOT RM is around 32 mol L^{-1} at $w_0 = 40$,[56] there is enough water to solvate the AOT headgroups and the CV molecules, and therefore, the ion pair formed in this condition, which has a λ_{max} of 598 nm, must be the SSIP and not the CIP. This conclusion is in accordance with the NMR data, which show that CV stays in the vicinity of the interface even at large w_0 values. An alternative explanation for the large λ_{max} of CV (much larger than the value of λ_{max} of CV in water) observed at high w_0 values would be the solvatochromic effect

(56) Srilakshmi, G. V.; Chaudhuri, A. *Chem.—Eur. J.* **2000**, *6*, 2847.

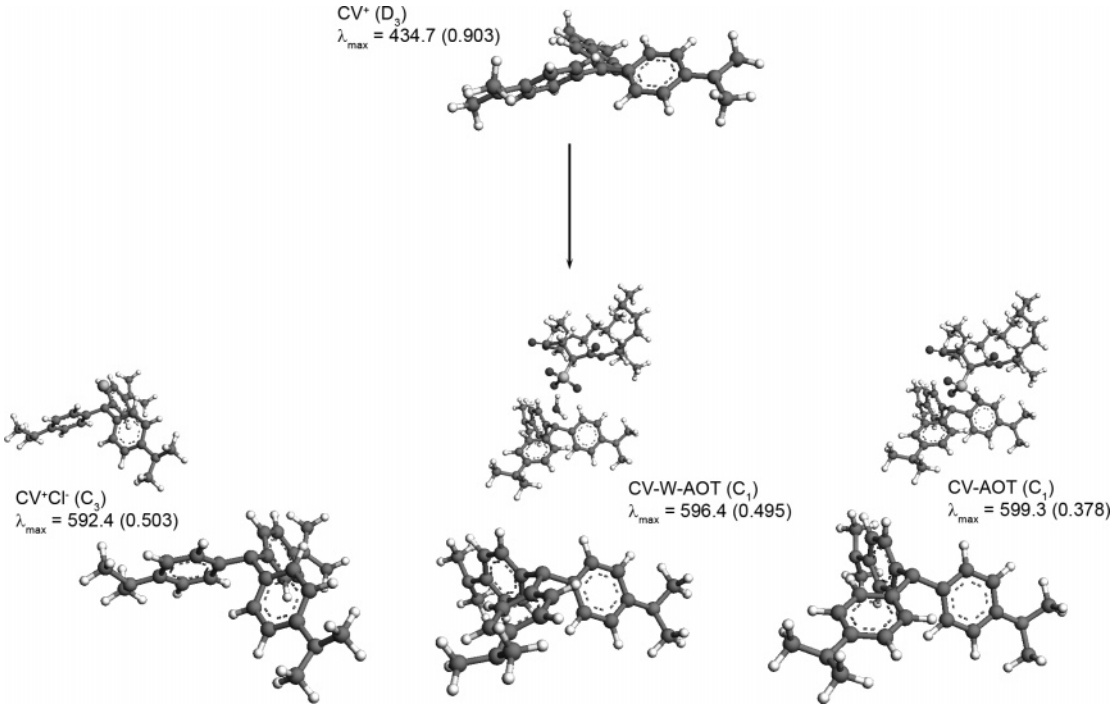

Figure 6. CV^+, CV^+Cl^-, $(CV^+)(H_2O)(AOT^-)$, and CV^+AOT^- optimized structures at the semiempirical PM3 level. Point groups and maximum absorption wavelengths (ZINDO-CI) are also shown. The calculated oscillator strength is shown in parentheses.

because the polarity of the interfacial region of the AOT RM is smaller than the polarity of water. However, this explanation does not proceed because, by decreasing the polarity of the medium, there is a decrease and not an increase in the value of λ_{max} of CV (λ_{max} in water is 590 nm and in ethanol 588 nm).

As mentioned earlier, the symmetry of CV is lowered as a consequence of contact ion pair formation. It has been shown that the solvation of CV by alcohols involves a change from a high-energy D_3 symmetry isomer (propeller-like structure) to a lower energy pyramidal isomer (C_3 symmetry).[57] Here we have investigated the effect of chloride and AOT on the maximum absorption wavelength, λ_{max}, of CV using a ZINDO-CI molecular orbital calculation based on PM3-optimized structures of CV, AOT, CV^+AOT^-, CV^+Cl^- and CV^+AOT^- CIPs, and $(CV^+)(H_2O)(AOT^-)$ SSIPs. As can be seen in Figure 6, in the absence of a counterion, CV assumes D_3 symmetry and a $\lambda_{max} = 434.7$ nm is observed, resulting from the HOMO−LUMO transition (singlet, 72 → 73, oscillator strength (*f*) 0.903). CV^+Cl^- has C_3 symmetry and a $\lambda_{max} = 592.4$ nm (HOMO−LUMO singlet, 72 → 73, $f = 0.503$). The CV^+AOT^- ion pair has C_1 symmetry and a calculated $\lambda_{max} = 599.3$ nm ((HOMO − 1)−LUMO singlet, 71 → 73, $f = 0.378$); therefore, this low-symmetry pair is further shifted to the red (ca. 7 nm), which is in accordance with the large value of λ_{max} observed in CV−AOT solutions in hexane and in AOT RMs. It is interesting to observe that the λ_{max} of the SSIP ($(CV^+)(H_2O)(AOT^-)$) is shifted to the blue in comparison with the CV−AOT CIP, with a λ_{max} of 596.4 nm ((HOMO − 1)−LUMO 71 → 73, $f = 0.495$). This is in agreement with the shift to the blue observed in the λ_{max} of CV in AOT RMs upon increasing the amount of water.

From these results, one can infer that the presence of both chloride and AOT as counterions of CV causes a decrease in its symmetry, which results in bathochromic shifts in λ_{max}. The reverse effect is observed when a water molecule is present between the ionic counterparts, i.e., a blue shift in comparison with the λ_{max} of CV CIPs. These results corroborate the interpretation that in AOT RMs at low and high w_0 values CV−AOT CIPs and SSIPs are, respectively, the major species present.

Discussion

The SAXS results show that the RM morphology is practically unaltered in the presence of CV. We shall infer that in the concentration range tested there is no kind of cooperative effect that could disturb a perceptible amount of RM interfaces.[36,43]

The NMR data show the interfacial localization of CV in close proximity to the SG group of AOT at low and high w_0 values. The interfacial localization of other positively charged molecules in AOT RMs had already been reported.[59,60] It has also been predicted in simulations by solvation dynamics in the water pool of AOT RMs at increasing values of w_0.[61]

The UV−vis spectroscopy data show that CV forms ion pairs with AOT in isotropic solution as well as in AOT RMs. The association constant between CV and AOT decreases with an increase in the solution dielectric constant, in analogy to other systems.[24,62−65] In AOT RMs, at low w_0 values CIPs were present and at high w_0 values SSIPs were present. The CV localization and ion pair formation were also confirmed by quantum chemical calculations.

As water is added to the RM and starts to hydrate the interface, it decreases the affinity between the SG group and CV. With an increase in w_0, there is a decrease in the concentration of CIPs while the SSIPs seem to be stable to w_0 values as large as ∼30.

(57) Maruyama, Y.; Ishikawa, M.; Satozono, H. *J. Am. Chem. Soc.* **1996**, *119*, 6257.
(58) Wittouck, N.; Negri, R. M.; Ameloot, M.; Deschryver, F. C. *J. Am. Chem. Soc.* **1994**, *116*, 10601.
(59) Raju, B. B.; Costa, S. M. B. *J. Phys. Chem. B* **1999**, *103*, 4309.
(60) Liu, D.; Ma, J.; Cheng, H.; Zhao, Z. *Colloid Polym. Sci.* **1998**, *276*, 610.
(61) Faeder, J.; Ladanyi, B. M. *J. Phys. Chem. B* **2005**, *109*, 6732.
(62) Matsumoto, H.; Yamamoto, R.; Tanioka, A. *J. Phys. Chem. B* **2005**, *109*, 14130.
(63) Fernandez, I.; Martinez-Viviente, E.; Pregosin, P. S. *Inorg. Chem.* **2004**, *44*, 5509.
(64) Cembram, A.; Bernardi, F.; Olivucci, M.; Garavelli, M. *Proc. Natl. Acad. Sci. U.S.A.* **2005**, *102*, 6255.
(65) Korppi-Tommola, J.; Yip, R. W. *Can. J. Chem.* **1981**, *59*, 191.

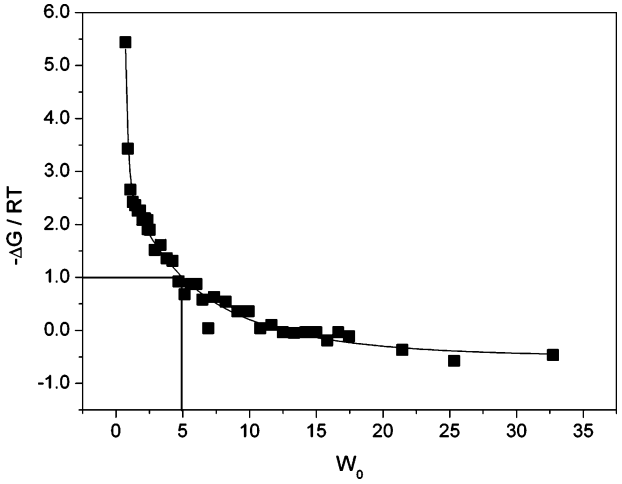

Figure 7. Gibbs free energy divided by the thermal energy at $T = 25$ °C ($RT = 2$ kJ mol^{-1}) as a function of w_0.

However, a question remains: is there a clear-cut water concentration in which the ion pairs change from CIPs to SSIPs in the AOT surface?

The ratio between the Gibbs free energy of the CIP association and the thermal energy at $T = 25$ °C as a function of w_0 is presented in Figure 7. It is clear that, with an increase in w_0, there is a sharp decrease in $-\Delta G/RT$ at low w_0 values (w_0 close to 1) whereas, for larger w_0 values, $-\Delta G/RT$ decreases slightly. This analysis suggests that there are major changes in the CV−AOT interactions when the first water molecules are added to the system. Note that, at $w_0 = 5$, i.e., there are five water molecules per AOT headgroup, the water solvation is enough to weaken the interactions between the ion pairs to a value equivalent to the thermal energy. Therefore, water is indeed very efficient in dissociating CV CIPs in AOT surfaces. Although the CIPs are easily broken, CV molecules stay in the vicinity of the AOT headgroups, forming SSIPs even at large water concentrations, which is in agreement with the low values of the ionic dissociation degree (α).[47,56]

The water inside an AOT RM can be well represented by three water populations:[16] trapped water molecules, localized up to 1 Å from the AOT interface, an intermediate layer of bound water, localized from 3 to 6 Å from the AOT interface, and the free or bulk water, localized at least 6 Å away from the AOT interface. Faeder and Ladanyi were able to distinguish the type of Na^+AOT^- ion pairs formed in the AOT interface as a function of w_0. They calculated that, at $w_0 = 1$, 80% of the ion pairs are CIPs and, at $w_0 = 10$, only 25% are still CIPs. Continuing these studies, Faeder et al. were able to show that K^+, because of its larger size compared with Na^+, is able to pack more efficiently in the RM interface and form a larger percentage of CIPs at low w_0 values.[22,66] Therefore, molecular simulation calculations show that, with an increase in the value of w_0, there is a decrease in the amount of CIPs giving place to the formation of SSIPs in AOT RMs. Similar results were obtained by Chorny and co-workers, who found that, in the presence of surfaces, SSIPs are more stable than CIPs.[23] In Monte Carlo simulations of NaI ion pairs in water clusters, Peslherbe and co-workers observed that while CIPs are present at small water/NaI molar ratios as low as 5, SSIPs are stable in water clusters at ratios as large as 50.[67]

Our experimental and quantum chemical calculation results are in agreement with those of the theoretical works cited above, indicating that ion pairs are mostly SSIPs in surfaces or interfaces at conditions in which the amount of water is larger than around five water molecules per charged surface group. It is important to notice that this condition includes all the surfactant aqueous solutions, oil-in-water microemulsions as well as water-in-oil microemulsions with w_0 larger than 5.

The formation of ion pairs is an important factor to define the structure and shape of supramolecular aggregates of amphiphile agents.[12,18−20] Geng and coauthors have precisely measured that in the vicinity of the sphere-to-rod transition of a gemini amphiphile solution there is a substantial increase in the surface counterion concentration (from 2.3 to 3.6 mol·L^{-1}) and a substantial decrease in the surface water concentration (from 35 to 17 mol·L^{-1}). On the basis of this and other data, they have proposed a new model for the balance of forces controlling morphological changes in colloids in which the aggregate morphology depends on the balance of the hydrophobic effect and hydration and ion pair formation. Formation of ion pairs and release of water allow tighter packing and the formation of cylindrical aggregates.[67] On the basis of our results, we conclude that the ion pairs formed in such conditions are SSIPs.

Acknowledgment. We thank FAPESP for financial support, a predoctoral research fellowship to C.S.O., and a postdoctoral research fellowship to E.L.B. and CAPES and CNPq for research grants. Theoretical calculations were performed using resources of the LCCA—Laboratory of Advanced Scientific Computation—of the University of São Paulo.

LA061117P

(66) Harpham, M. R.; Ladanyi, B. M.; Levinger, N. E. *J. Phys. Chem.* **2005**, *109*, 16891.

(67) Peslherbe, G. H.; Ladanyi, B. M.; Hynes, J. T. *J. Phys. Chem. A* **2000**, *104*, 4533.